

Supplementary Information

Plasmonic TiN-Supported CuPd Alloy for Highly Selective and Base-Free Photocatalytic Glaser Homocoupling

Huijie Hao,^a Yaying Li,^a Ting Han^b and Qi Xiao*^a

^a State Key Laboratory of Advanced Fiber Materials, College of Materials Science and Engineering, Donghua University, Shanghai 201620, China

^b Instrument Analysis Center, Tongji University, Shanghai 200092, China

Email: qi.xiao@dhu.edu.cn

Experimental section

Materials

Titanium nitride (TiN) and acetonitrile were purchased from Aladdin Scientific Corp. Copper nitrate hydrate ($\text{Cu}(\text{NO}_3)_2 \cdot 3\text{H}_2\text{O}$) was purchased from Energy Chemical Co., Ltd. Phenylacetylene was purchased from Macklin Biochemical Technology Co., Ltd. Palladium (II) chloride (PdCl_2) was purchased from Sigma-Aldrich.

Characterization.

High-resolution transmission electron microscopy (HRTEM) images and energy-dispersive X-ray spectroscopy (EDS) images were obtained on a JEOL JEM-2100F instruments. Powder X-ray diffraction (XRD) results were acquired by a Miniflex 600. X-ray photoelectron spectroscopy (XPS) analysis was performed using Shimadzu AXIS Supra. The X-ray absorption spectroscopy (XAS) measurements were obtained on beamline BL13SSW at the Shanghai Synchrotron Radiation Facility. XAS data processing followed the standard procedures using the ATHENA and ARTEMIS programs. The UV-vis absorption spectra were obtained by a UV-2600 diffuse reflectance spectroscopy. The metal loading amounts of the samples were analyzed on Prodigy plus ICP-OES. Electron paramagnetic resonance (EPR) was obtained by a JES-X320.

Synthesis of CuPd/TiN catalysts

The CuPd/TiN catalysts were prepared as follow: A total of 100 mg of commercial TiN was uniformly dispersed in 4 mL of deionized water. To this dispersion, a mixed metal precursor solution (94 μL of 0.01 M PdCl_2 and 1.56 mL of 0.02 M $\text{Cu}(\text{NO}_3)_2$) was added. The mixture was ultrasonicated for 10 minutes to ensure thorough mixing, followed by rapid freezing in liquid nitrogen to form a TiN-coated ice template incorporating the metal ions. The frozen sample was then subjected to vacuum freeze-drying to remove the ice matrix, yielding the catalyst precursor. Finally, the precursor was calcined at 400 °C for 1 h under an Ar/ H_2 mixed gas atmosphere, with a heating rate of 5 °C/min, to obtain the $\text{Cu}_2\text{Pd}_{0.1}/\text{TiN}$ catalyst. Other catalysts with different metal ratios were prepared using the same procedure.

Experimental process for Glaser homocoupling reaction

In a typical photocatalytic Glaser homocoupling reaction, 15 mg of the catalyst was added to a solution of 0.01 mmol phenylacetylene in 5 mL of acetonitrile. The reaction was carried out in a quartz glass reactor under air atmosphere, with the temperature maintained at 35°C by circulating cooling water. The system was then transferred into a multi-channel photochemical reaction system (PCX-50C, Beijing Perfect light Technology Co., Ltd.) and irradiated under white LED light. After the reaction, the products were quantitatively analyzed by gas chromatography (GC-MS, Agilent 8860-5977B). Phenylacetylene conversion and 1,4-diphenylbutadiyne selectivity were calculated with the equations shown below:

$$\text{conversion}(\%) = \frac{(\text{mmol of phenylacetylene converted})}{(\text{mmol of initial phenylacetylene})} \times 100$$

$$\text{selectivity(\%)} = \frac{(\text{mmol of 1,4 - diphenylbutadiyne})}{(\text{mmol of phenylacetylene converted})} \times 100$$

Electron Paramagnetic Resonance (EPR)

The signals of free radicals were obtained on electron paramagnetic resonance (EPR) spectrometer (JES-X320) using the 5,5-dimethyl-1-pyrroline N-oxide (DMPO) as the trapping agent. Specifically, for the test of $\cdot\text{O}_2^-$, 15 mg catalysts were dispersed in DMPO/methanol solution. The signals were collected under dark and light irradiation ($\lambda > 400$ nm).

Supporting Figures

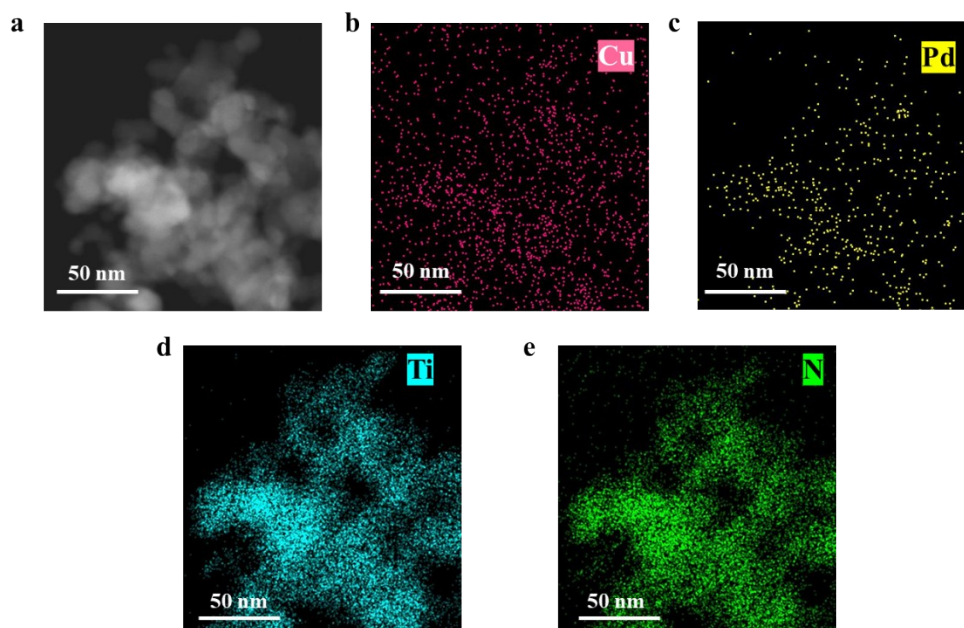


Fig. S1 (a) TEM image and (b-e) EDS elemental mapping of $\text{Cu}_2\text{Pd}_{0.1}/\text{TiN}$.

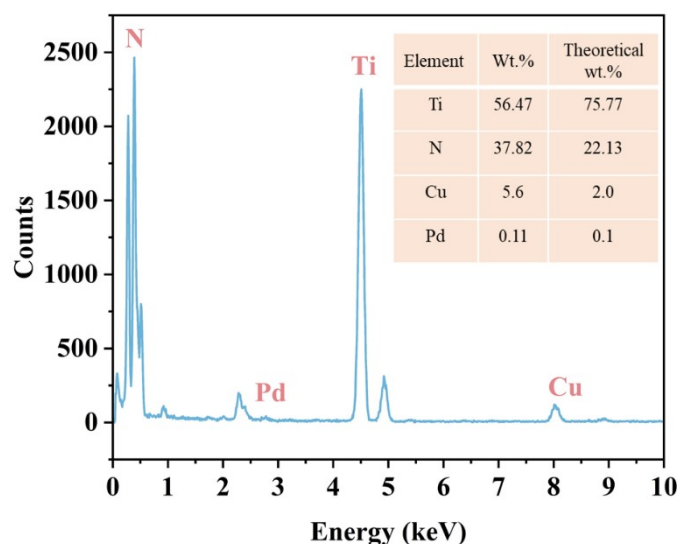


Fig.S2 EDS spectrum of $\text{Cu}_2\text{Pd}_{0.1}/\text{TiN}$.

The theoretically designed load on the TiN support was 2.0% Cu and 0.1% Pd, while the measured results were Cu (5.60%), Pd (0.11%), Ti (56.47%), and N (37.82%). The Pd content (0.11%) closely matches the theoretical value (0.1%), indicating accurate control of Pd loading, whereas the Cu content (5.60%) is significantly higher than the theoretical value (2.0%), which may be due to a higher Cu loading at that site; however, combined with ICP-OES data analysis, the metal loading amount is relatively accurate. The mass ratio of Ti to N (~ 1.49) is lower than the theoretical ratio of TiN (~ 3.42), indicating that the sample is relatively thin, allowing the electron beam to penetrate the TiN layer and excite the N-containing substrate or contamination layer, resulting in an overestimation of N content and dilution of Ti content.

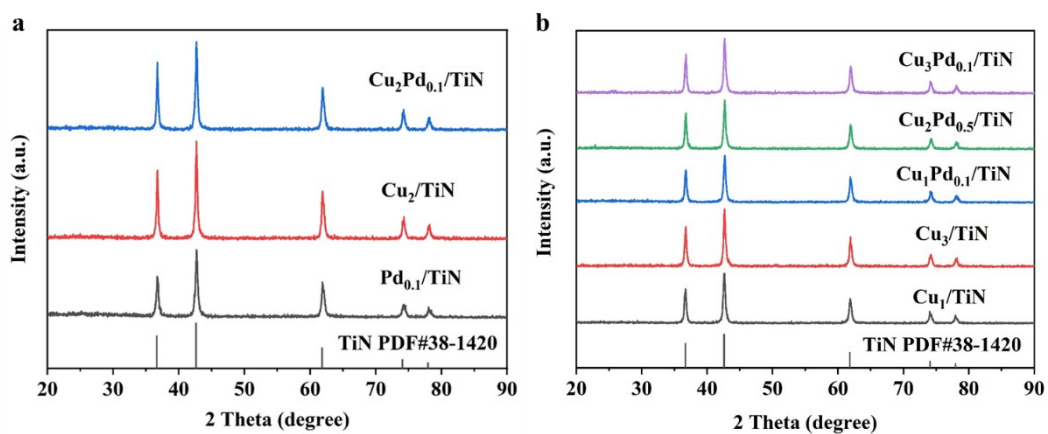


Fig. S3 (a, b) XRD patterns of CuPd/TiN samples with different metal ratios.

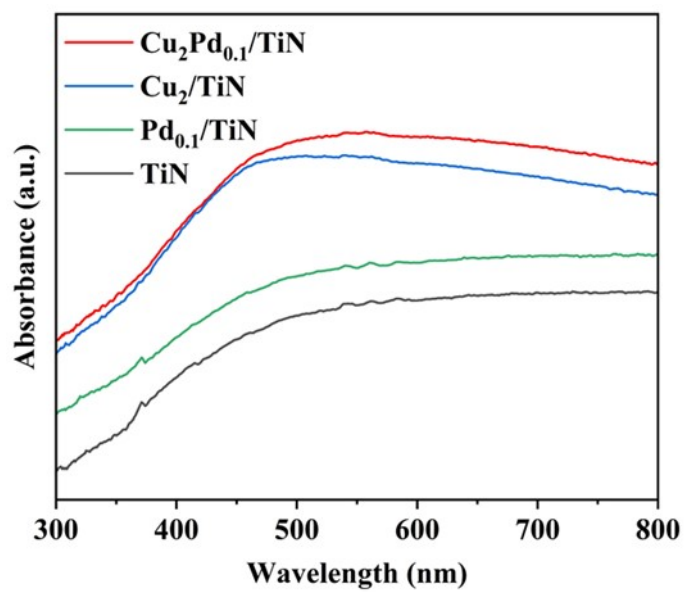


Fig. S4 UV-vis absorption spectra of different catalysts.

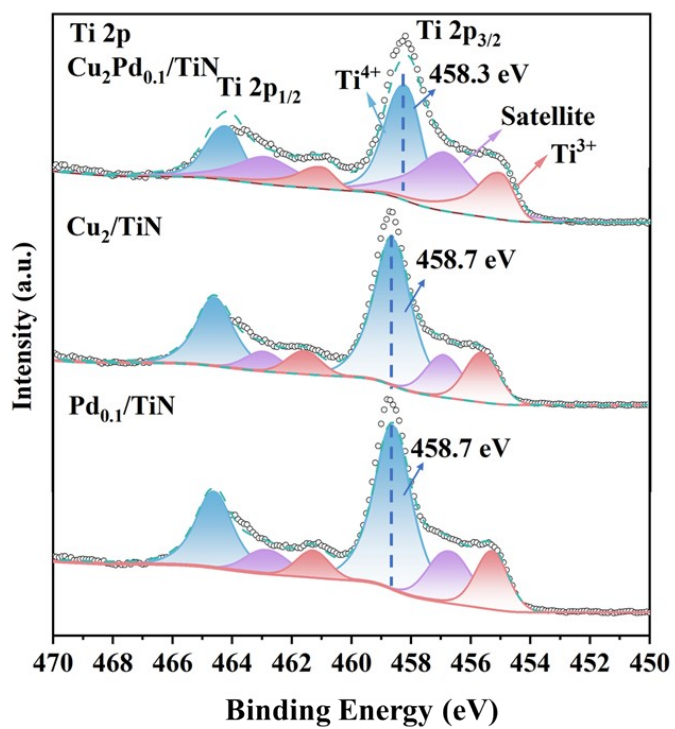


Fig. S5 Ti 2p XPS spectra of Cu₂Pd_{0.1}/TiN, Cu₂/TiN and Pd_{0.1}/TiN.

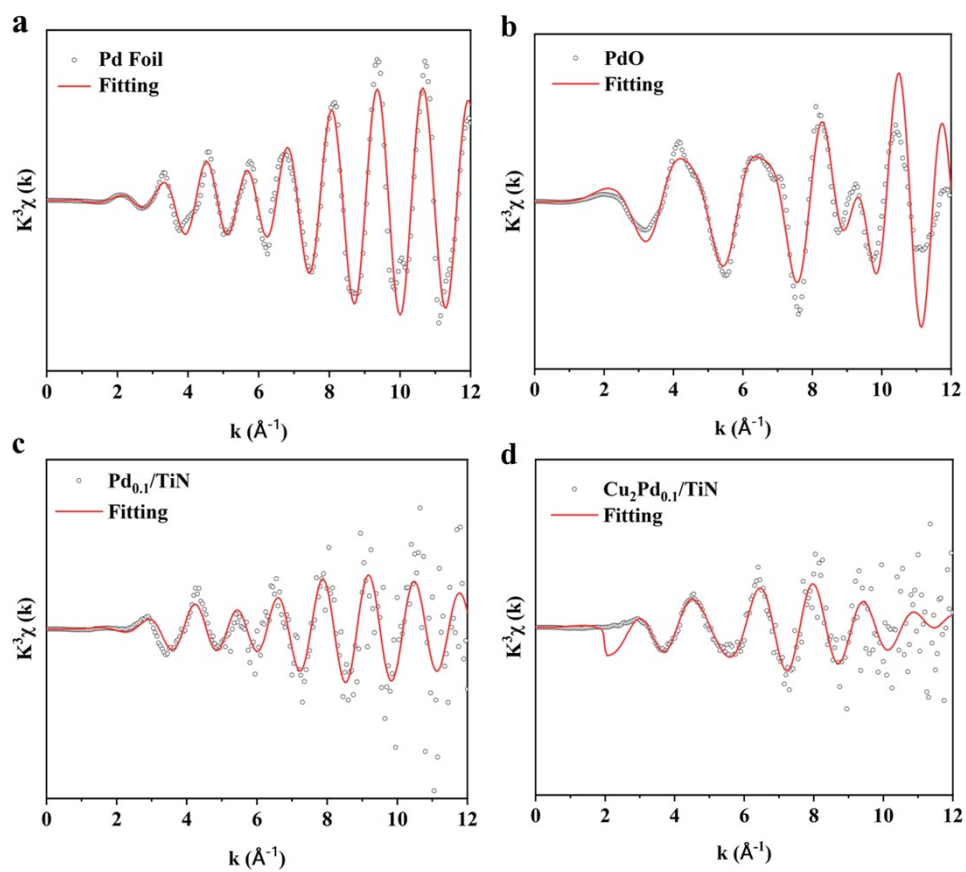


Fig. S6 K-space curves of (a) Pd Foil, (b) PdO, (c) Pd_{0.1}/TiN, and (d) Cu₂Pd_{0.1}/TiN

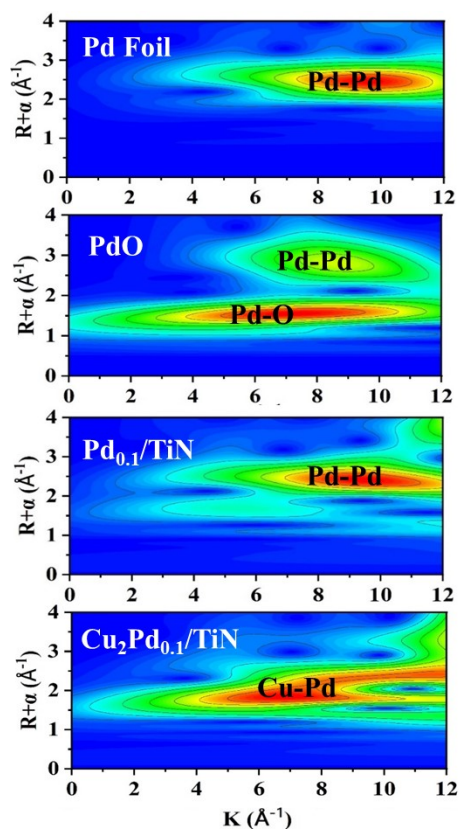


Fig. S7 Pd K-edge WT-EXAFS spectra of Pd Foil, PdO, Pd_{0.1}/TiN, Cu₂Pd_{0.1}/TiN.

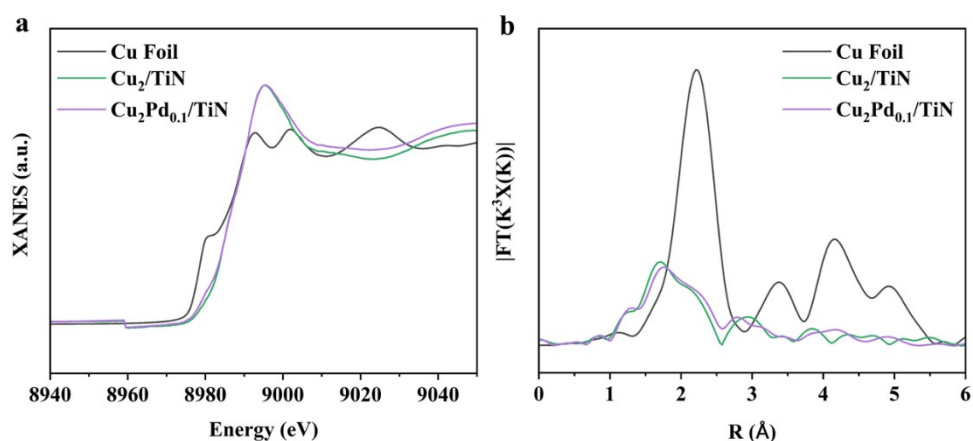


Fig.S8 (a) Normalized Cu K-edge XANES spectra, (b) FT-EXAFS fitting curves of Cu Foil, Cu₂/TiN, and Cu₂Pd_{0.1}/TiN.

Due to the larger amount of Cu loading, the Cu K-edge EXAFS signal is statistically dominated by the bulk Cu–Cu coordination environment. Consequently, the subtle structural changes occurring at the limited number of Cu–Pd interfaces are largely masked by the majority of Cu–Cu bonds (Fig. S8). In contrast, the Pd K-edge EXAFS serves as a far more sensitive probe for confirming the local coordination environment of the synergistic alloy phase in this specific low-Pd system.

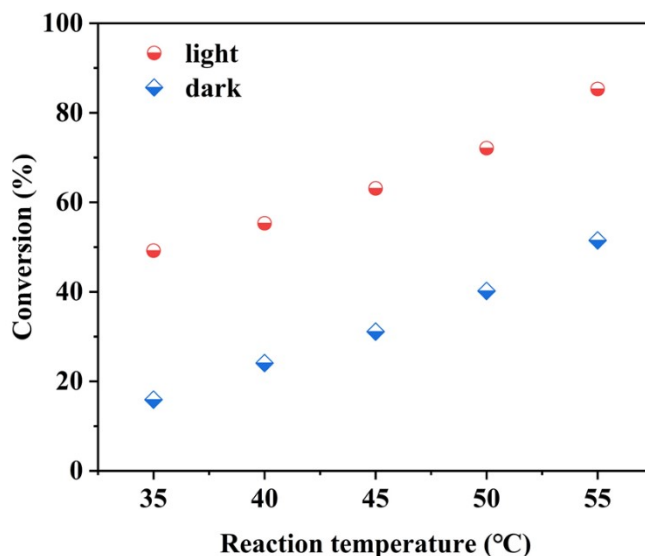


Fig. S9. The catalytic activity of the Glaser coupling reaction under light irradiation and in the identical dark conditions conducted at different reaction temperatures. Reaction conditions: 15 mg catalyst; 0.1 mmol phenacetylene; 5 mL acetonitrile; reaction time 4 h.

To distinguishing between plasmonic photothermal effects and hot-carrier-driven photocatalytic processes for understanding the reaction mechanism. We systematically monitored the actual temperature of the reaction system under visible light irradiation. The measured temperatures were 35.5°C, 40.2°C, 46.1°C, 50.8°C, and 55.6°C, showing no significant localized overheating beyond the set parameters. Importantly, at each equivalent temperature, the conversion under light irradiation was significantly higher than that in the dark (Fig. S9). This result demonstrates that thermal energy alone, whether from external heating or internal photothermal conversion, is insufficient to drive the high-efficiency Glaser coupling observed. While minor photothermal heating might exist, the dramatic enhancement in catalytic performance is fundamentally attributed to the catalytic pathway triggered by photogenerated hot electrons from the plasmonic CuPd/TiN catalyst, rather than a simple photothermal effect.

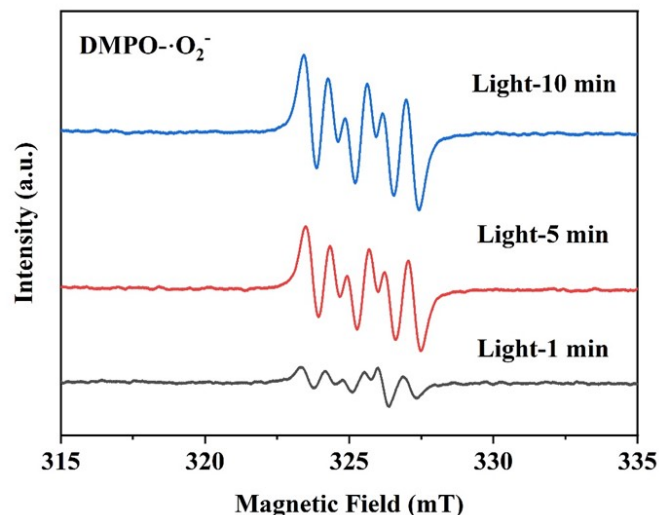


Fig. S10 DMPO spin-trapping EPR spectra of Cu₂Pd_{0.1}/TiN under light irradiation

While $\cdot\text{O}_2^-$ is identified as a key active radical species via EPR (Fig. 3b), it is an intermediate rather than the terminal reduction product. In our system, the CuPd alloy promotes a stepwise, multi-electron reduction of O₂ that sequentially consumes the protons (H⁺) released from the C–H activation of phenylacetylene on Cu sites. The integrated pathway is as follows:

- (1) $\text{O}_2 + \text{e}^- \rightarrow \cdot\text{O}_2^-$
- (2) $\cdot\text{O}_2^- + \text{e}^- + 2\text{H}^+ \rightarrow \text{H}_2\text{O}_2$
- (3) $\text{H}_2\text{O}_2 + 2\text{e}^- + 2\text{H}^+ \rightarrow 2\text{H}_2\text{O}$

According to the stoichiometry of Glaser coupling ($2\text{R}-\text{C}\equiv\text{C}-\text{H} + 1/2\text{O}_2 \rightarrow \text{R}-\text{C}\equiv\text{C}-\text{C}\equiv\text{C}-\text{R} + \text{H}_2\text{O}$), the oxidation of 2 moles of phenylacetylene yields 2 electrons (e⁻) and 2 protons (H⁺), which exactly matches the requirement for reducing 0.5 moles of O₂ to H₂O.

Supporting Tables

Table S1. ICP analysis results of the CuPd/TiN catalysts with different metal ratios.

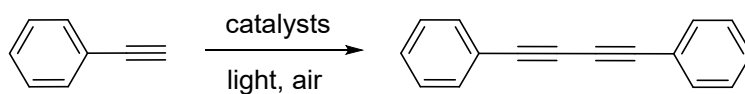
| Catalyst | Actual Cu loading (wt.%) | Nominal Cu loading (wt.%) | Actual Pd loading (wt.%) | Nominal Pd loading (wt.%) |
|--|--------------------------------|---------------------------------|--------------------------------|---------------------------------|
| Cu ₁ /TiN | 1.02 | 1.00 | - | - |
| Cu ₂ /TiN | 1.86 | 2.00 | - | - |
| Cu ₃ /TiN | 2.68 | 3.00 | - | - |
| Cu ₁ Pd _{0.1} /TiN | 0.71 | 1.00 | 0.09 | 0.10 |
| Cu ₁ Pd _{0.5} /TiN | 0.83 | 1.00 | 0.49 | 0.50 |
| Cu ₂ Pd _{0.1} /TiN | 1.88 | 2.00 | 0.09 | 0.10 |
| Cu ₂ Pd _{0.5} /TiN | 1.97 | 2.00 | 0.47 | 0.50 |
| Cu ₃ Pd _{0.1} /TiN | 2.68 | 3.00 | 0.10 | 0.10 |
| Cu ₃ Pd _{0.5} /TiN | 2.64 | 3.00 | 0.47 | 0.50 |

Table S2. EXAFS fitting parameters at the Pd K-edge of Pd Foil, PdO, Pd_{0.1}/TiN and Cu₂Pd_{0.1}/TiN.

| Sample | Shell | CN | R (Å) | $\sigma^2(10^{-3}\text{Å}^2)$ | ΔE_0 (eV) | R-factor |
|--|-------|---------------|-----------------|-------------------------------|-------------------|----------|
| Pd Foil | Pd-Pd | 12 | 2.86 ± 0.01 | 6.91 | 3.8 | 0.017 |
| PdO | Pd-O | 2.7 ± 0.8 | 1.76 ± 0.03 | 0.86 | 4.1 | 0.010 |
| Pd _{0.1} /TiN | Pd-Pd | 4.9 ± 1.0 | 2.74 ± 0.01 | 7.79 | 5.7 | 0.006 |
| Cu ₂ Pd _{0.1} /TiN | Cu-Pd | 9.7 ± 1.1 | 2.55 ± 0.04 | 17.89 | 12.3 | 0.029 |
| | Pd-Pd | 6.1 ± 0.8 | 2.64 ± 0.13 | 15.69 | | |

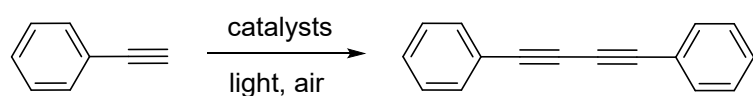
The value of S_0^2 is obtained from the fitting for Pd Foil (Pd 1.00). CN is the coordination number. R is interatomic distance (the bond length between central atoms and surrounding coordination atoms). σ^2 is Debye-Waller factor (a measure of thermal and static disorder in absorber scatter distance). ΔE_0 shift is edge-energy shift (the difference between the zero kinetic energy value of the sample and that of the theoretical model). R factor is used to value the goodness of the fitting.

Table S3. Performance diagram of other catalyst photocatalytic Glaser homocoupling reaction



| Entry | Catalyst | Light | | Dark | |
|-------|--|----------------|-----------------|----------------|-----------------|
| | | Conversion (%) | Selectivity (%) | Conversion (%) | Selectivity (%) |
| 1 | TiN | 0 | - | 0 | - |
| 2 | Cu ₁ /TiN | 0 | - | 0 | - |
| 3 | Cu ₂ /TiN | 71.3 | 100 | 60.7 | 100 |
| 4 | Cu ₃ /TiN | 30.4 | 100 | 30.1 | 100 |
| 5 | Pd _{0.1} /TiN | 0 | - | 0 | - |
| 6 | Pd _{0.5} /TiN | 0 | - | 0 | - |
| 7 | Cu ₂ Pd _{0.1} /TiN | 99.1 | 100 | 41.8 | 100 |

Reaction conditions: 15 mg catalyst; 0.1 mmol Substrate; 5 mL Acetonitrile; air; 35°C; reaction time (8 h); white LED (0.5W/cm²). Conversions were determined by using GC-MS.

Table S4. Solvent optimization of the photocatalytic Glaser homocoupling reaction.

| Entry | Catalyst | Solvent | Conversion (%) | Selectivity (%) |
|-------|--|------------------------|----------------|-----------------|
| 1 | Cu ₂ Pd _{0.1} /TiN | Acetonitrile | 99.1 | 100 |
| 2 | Cu ₂ Pd _{0.1} /TiN | Ethanol | 1.7 | 100 |
| 3 | Cu ₂ Pd _{0.1} /TiN | Isopropanol | 12.8 | 100 |
| 4 | Cu ₂ Pd _{0.1} /TiN | Dichloromethane | 16.4 | 100 |
| 5 | Cu ₂ Pd _{0.1} /TiN | N, N-Dimethylformamide | 0 | - |
| 6 | Cu ₂ Pd _{0.1} /TiN | Methanol | 4.6 | 100 |
| 7 | Cu ₂ Pd _{0.1} /TiN | 1,4-Dioxane | 0 | - |

Reaction conditions: 15 mg Cu₂Pd_{0.1}/TiN; 0.1 mmol Phenylacetylene; 5 mL solvent; air; 35°C; reaction time (8 h); white LED (0.5W/cm²). Conversions were determined by using GC-MS.